Experimental and computational surface roughness analysis of aluminium silicon 12 (AlSi12) produced by powder bed fusion for transport applications

Alliance Gracia Bibili Nzengue[1]*, *Khumbulani* Mpofu[1], *Ntombizodwa Ruth* Mathe[2] and *Rumbidzai* Muvunzi[3]

[1]Tshwane University of Technology, Industrial Engineering Department, Staatsartillerie Rd, Pretoria West, Pretoria, South Africa
[2]Council for Scientific and Industrial Research, Photonics Centre, Meiring Naudé Road, Brummeria, Pretoria, South Africa
[3] Cape Peninsula University of Technology, Industrial and Systems Engineering Department, Robert Sobukwe Rd, Bellville South Industrial, Cape Town, South Africa

Abstract. Surface roughness influences the mechanical performance of a part. A rougher surface is prone to cracks and corrosion due to increased friction and harsh environments in transport applications. Given that surface irregularities are difficult to control, post-processing is critical to improving the surface roughness. In this study, post-processing treatment such as the vibratory polishing process was used with different media to investigate the surface roughness parameters, arithmetic mean roughness (Ra) and the maximum depth of the roughness valley (Rv) of AlSi12 produced by the powder bed fusion technique. Two measuring instruments; Gwyddion and Stylus Profilometer were used for the collection of data. The analysis of the results demonstrated that the measurements taken from the experimental setup using the stylus profilometer are complementary with those taken from the computational using the Gwyddion software. The findings suggested that the vibratory polishing technique significantly reduced the surface roughness of additively manufactured AlSi12. This study provides insights into ensuring the performance and reliability of component surface properties for applications in the transport industry.

1 Introduction

Aluminium (Al) alloys have garnered a large amount of interest for applications in the transportation industry due to their corrosion resistance and high strength-to-ratio [1]. Al alloys have become increasingly used in the replacement of cast iron and steel materials, drawing on their lightweight properties [2].

* Corresponding author: alliancebibili@gmail.com

The processing of Al alloys such as AlSi12 with powder bed fusion techniques has been challenging due to their poor flowability and low density [3]. These latter properties increase the likelihood of defects such as balling, porosity, and cracks that consequently affect the surface roughness. As a result, the microstructure of the material is also altered. Furthermore, considering the complexity of the powder-bed fusion manufacturing technique, there is a probability that the desired surface roughness is not obtained [4]. Powder bed fusion techniques, such as Selective Laser Melting (SLM), are very prone to surface quality defect challenges [5]. This is due to the turbulence in the melt pool that initiates uneven solidification of the melted material, and the high level of energy input that creates unmelted powder particles on the contour of the part [6]. This results in a poorer surface quality of the part, reduced strength and resistance to corrosion, and wear.

Surface roughness is a critical element of the surface quality of fabricated parts because it influences the service life of the parts. Surface roughness also affects the mechanical properties of the part when in service [7]. In the transportation industry such as aerospace, the surface roughness specification is strict and should be below 3.20 μm for functional components and lower than 1.6 μm where fatigue is critical [6]. This has prompted great efforts to explore approaches for improving surface quality. Several investigations involved the reduction of defects such as balling and unmelted powder generated during processing, which led the authors to study the impact of surface roughness on the fatigue life of AlSi10Mg material [7, 8]. A relatively well-documented aspect is the study of the effect of the SLM processing parameters on surface roughness [3, 9, 10]. These studies used mathematical modelling and experimentation to assess and predict the desired surface quality and geometry accuracy of the parts or specimens fabricated.

In an experimental sense, the use of technologies has provided alternatives to improve the surface roughness at the post-processing stage. Since conventional machining can be complex for intrinsic parts structure, shot peening, electrochemical polishing, laser ablation, chemical etching, remelting -polishing and use of abrasive fluids have been studied [11-15]. These studies reported that the quality of the surface improved by using these techniques. Previous studies have also reported the use of vision-based techniques to prevent defects that affect the surface [16]. However, the approach works with sensors and is used for in situ monitoring, which involves data processing and a large number of trial-and-error tests to achieve accurate surface quality. A significant drawback of the aforementioned approaches is the high cost associated with the processes. Post-processing activities, in general, are expensive and time-consuming. Given these challenges, vibratory grinding has been adopted as an alternative technique due to its capabilities of preserving the geometric accuracy and characteristics of the part. Despite its benefits, there are insufficient studies on the use of this method [15].

To determine the effectiveness of the vibratory grinding method, a roughness measurement is needed. Parameters such as speed and time can be varied to obtain the desired surface roughness values. Various instruments are available for surface roughness measurements, for example, atomic force microscopy (AFM), confocal laser scanning microscope, scanning electron microscope (SEM), and profilometers. Additionally, open-access software such as Gwyddion can be exploited for these measurements [17]. Among the various metrics for surface roughness, the mean deviation R_a is one of the most widely used measurements [18]. Several studies have focused on mathematical models to predict surface roughness, including parameters such as geometrical dimensions and profiled surfaces [19]. There is a need to correlate the experimental results with computational predictions to enhance the accuracy and reliability of these models.

Therefore, this study investigates the influence of polishing on the top layer of the surface roughness. It includes a comparative analysis of the surface parameters measured using an optical profilometer and Gwyddion software after processing samples with the vibratory

grinding method. The surface parameters were analysed to achieve the requirements of the transport industry.

2 Methodology

2.1 Sample fabrication procedure and experimental measurement

The material used for the fabrication of the samples was AlSi12 alloy. It was used as commercially procured and was processed through SLM on an in-house machine (humming bird) at the Council for Scientific and Industrial Research (CSIR). The samples were built under the same conditions with a laser power of 1400W, layer thickness of 0.05 mm, hatch spacing of 0.1 mm, and an energy density of 186.67j/mm^3.

Post fabrication, the samples underwent polishing using a vibratory finishing system equipped with two rotating shafts. This process consisted of three phases each using different types of media. In the first phase, rough polishing was achieved with ceramic media (10x10 mm angle cuts). The second phase utilised plastic media (pyramid cut 6x6 mm) for low abrasion, while the third phase combined zirconia balls (4x4 mm) with plastic media to achieve a smoother surface. The plastic media was reported to be the first choice for aluminium materials based on recommendations from a previous study on AlSi10Mg [20]. Hence, the surface roughness study analysis focused on the two last phases, namely B and C in this study (with A referring to as-built condition).

The rotating shafts were filled to 75% capacity and drops of LC13 along with some water were added to create an appropriate viscosity during the vibratory process. The system's speed was varied to 160 rpm, 170 rpm and 180 rpm with a constant processing time of 3 hours. The average values for each speed were considered for analysis and presented in the results section.

After completing the polishing process, a Taylor Hobson Surtronic S-100 series profilometer - S-128 presented in Fig. 1., which comprises a stylus arm, was utilised for the measurement of the surface roughness following international procedures.

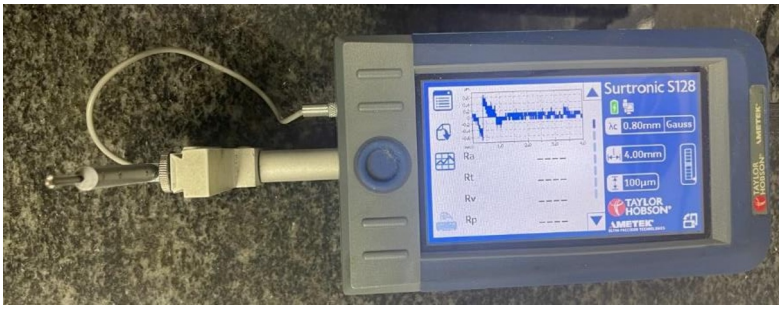

Fig. 1. Roughness tester: Taylor Hobson Surtronic S-100 series—S-128

The instrument recorded the surface roughness for the as-built condition and after polishing conditions (B and C). This was done to observe the effect of the polishing profile on the surface quality. The roughness measurements consisted of parameters such as the arithmetic mean roughness (R_a) and the maximum depth of the roughness valley (R_v).

The roughness average R_a is determined as follows:

$$R_a = \frac{1}{N_x N_y} \sum_{i=1}^{N_x} \sum_{j=1}^{N_y} |Z(i,j) - Z_{mean}| \quad (1)$$

Given that N_x and N_y are points along the X and Y axes of the image of analysis with i and j as the scanning point to be measured, Z_{mean} is the mean height and $Z(i,j)$ the height of the points [17].

$$R_v = |min\, z(x)| \quad (2)$$

$Z(x)$ represents the maximum valley of the roughness profile in terms of the depth of the scanning point along the length.

2.2 Computational measurement

The computational measurement was conducted using Gwyddion, an open software that allows the collection of microscopic data from the analysis of the scanning probe [21]. Scanning electron microscopy (SEM) images were inserted into the software to visualise the surface roughness and edge detection. The SEM images were uniformly using a magnification of 30 with a 500 µm resolution. The segmentation of the surface to be analysed was measured throughout the sample image, and statistical functions included in the software generated the results. The quantitative results are given in spatial, hybrid, functional, and amplitude. The amplitude functions comprised various elements such as the average roughness (Ra), the maximum depth of the roughness valley (Rv), the mean square roughness of the root (Rq), skewness (Rsk), kurtosis (Rku), and average waviness (Wa) to name a few [21]. For this study, Ra is considered due to its historical data availability and standards established worldwide. Rv is also studied to determine the peak depth of valleys of each profile. Moreover, it should be noted that these parameters are not affected by the contamination or noise that results from the measurement [22]. The default mask settings were applied to maintain the images in their original state, and lines were drawn on the images to obtain the measurement readings.

3 Results and discussion

3.1 Experimental analysis

The experimental surface measurements of AlSi12 emphasised the measurements of key parameters R_a and R_v. Figure 2 presents the values of the R_a with A representing the as-built values, while B the values after polishing with the plastic media. C the values after polishing with the combined zirconia balls and plastic media. All the R_a values were recorded at different speeds of 160 rpm, 170 rpm and 180 rpm at a constant time of 3 hours [20].

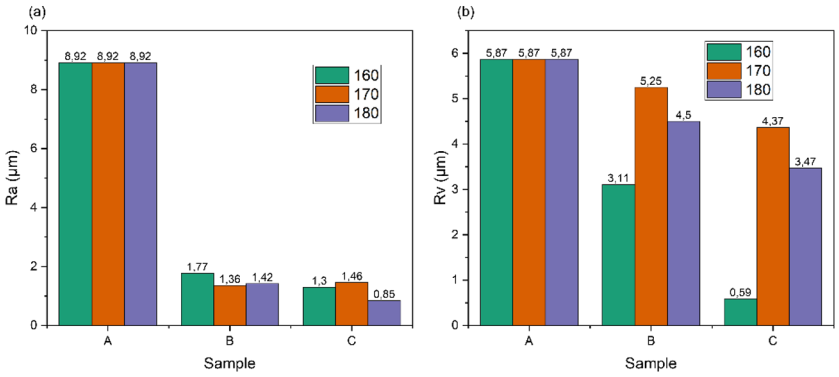

Fig. 2. Experimental Roughness measurements for AlSi12. (a) R_a values and (b) R_v values (A- as-built, B-after plastic media, C-after Zirconia mixed with plastic).

From Fig. 2 (a), it was observed that the combination of zirconia and plastic media led to a decreased surface roughness of 80% at 180 rpm speed. The R_a at 170 rpm is, however, slightly increasing this might be due to a few micro-sleets on the surface. During the process, the sample and media grind against each other; the media could be found attached to the tumbler, which reduced the effect of the media on the samples. The impact of the surface deformation per interaction in the tumbler was due to the lubrification and temperature initiated by the speed. Moreover, the surface polishing demonstrated that the different media affected the surface quality. The high surface roughness R_a of the as-built 8.92 µm dropped to 0.85 µm after the final polishing phase in C. Increasing the speed in the B and C phases enhances the efficiency of the grinding process [23]. This has significantly affected the rate of removal of the molten particles on the surface and smoothened the surface of AlSi12. This effect could be attributed to the fact that the samples were fabricated with a high energy density, which entails that the powder fused during the fabrication process. In addition, the AlSi12 is considered a softer material which can contribute to its surface morphology improvement.

In Fig.2 (b), the maximum valley depth R_v shows the as-built (5.87 µm) and a variation of the values obtained. At speeds of 170 rpm to 180 rpm, an expansion from 17% to 23% is observed from phase B to C. A significant decline is recorded at a speed of 160 rpm, which shows that the deepest valley on the surface is smoother. The low percentage of 17% reduction can be attributed to the fact that the material was not stress-relieved [23]. Controlling R_v ensures that the material weakness can be evaluated, and better performance is achieved for the application.

3.2 Computational analysis

Fig. 3 depicts the SEM micrographs of AlSi12 at a magnification of X30 to have a full view of the surface. The surface morphology measurements were conducted using Gwyddion software. The height values of the surface are the chromaticity in the map. The SEM analysis of the B and C samples revealed finer grains in their surface microstructure. It is reported that finer grain morphology contributes to lower surface measurement, whereas surfaces with coarser grain unveil irregularities leading to rougher surface textures and consequently to a higher surface roughness measurement [1].

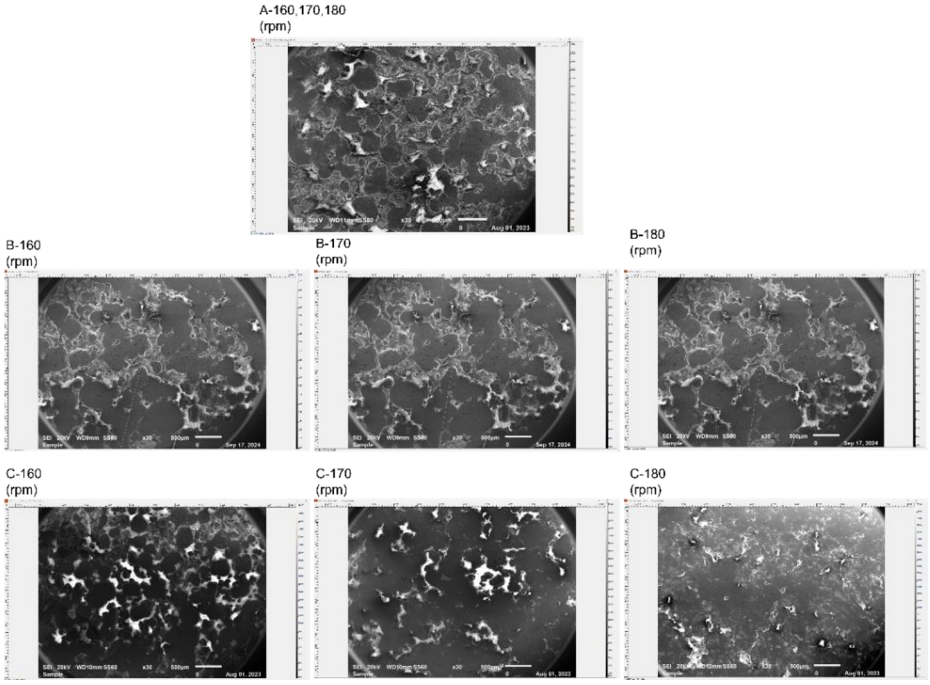

Fig. 3. SEM micrographs of AlSi12 used for measurements on Gwydion (A- as-built, B-after plastic media, C- after zirconia mixed with plastic).

The microstructures of the samples at the as-built condition show larger particles, while at phase B, some satellites at a minimal size are present. In phase C, a smoother surface is depicted. This is evidenced by the larger surface particles being removed. The white spots observed are the residuals of the solution deposited on the surface.

The arithmetic mean roughness Ra was further recorded from the SEM images and is presented in Fig.4. At a speed of 160 rpm it is described that the Ra decreased from the as-built condition. However, when comparing the B and C phases the speed of 160 rpm yielded the higher Ra values that are singularised by the graph's patterns. The high peaks at 170 rpm and 180 rpm suggest that there was a decrease of about 91% in the surface roughness in both phases of B and C.

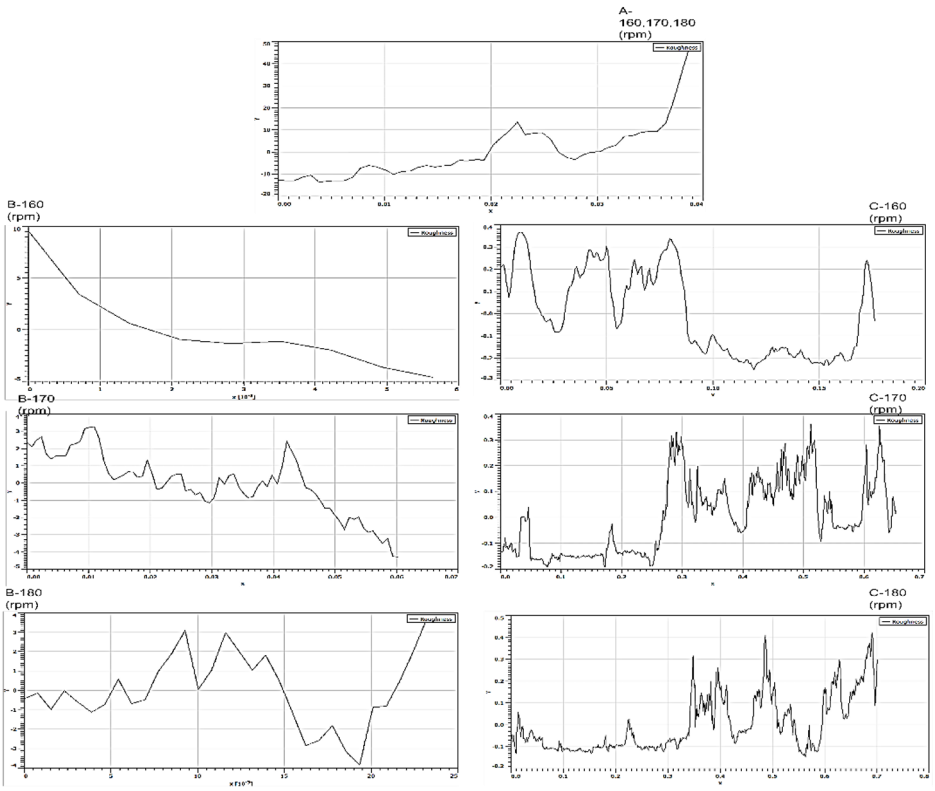

Fig. 4. Surface roughness of AlSi12 measured on Gwyddion (A- as-built, B-after plastic media, C - after zirconia mixed with plastic).

The variability of the peaks (C-170,180 rpm) may indicate the inconsistencies in the localised measured surface. This could be potentially caused by inclusions or the residual deposited solution on the surface. Overall, the Ra graph patterns have a downward inclination, which implies a gradual smoothening of the surface. This implies that the polishing process in two phases significantly lessened the surface irregularities by minimising the deepest valleys and sharp peaks. The improved surface integrity is crucial for AlSi12 application in the transport sector as it enhances its capability to resist corrosion and wear [7].

The Rv values in Fig.5. correlate with the Ra results and establish the considerable effect of the surface polishing process on the quality of the surface finish.

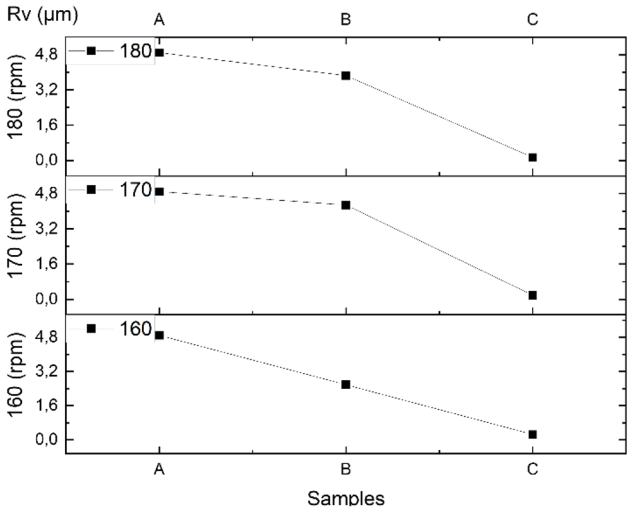

Fig. 5. Maximum valley depth of AlSi12 from Gwyddion (A- as-built, B-after plastic media, C-after zirconia mixed with plastic).

4 Comparative analysis of experimental and computational values

The experimental calculated R_a in the B phase conditions in the respective values of 1.77 µm, 1.36 µm and 1.42 µm is in close correlation with the computational obtained values of 1.81 µm, 1.37 µm and 1.43 µm under 160, 170 and 180 rpm. However, in the second phase C, there is a discrepancy of the obtained values in the experimental as compared to the computational measurements at the varied speeds. The experimental values were 1.3 µm, 1.46 µm and 0.85 µm; while computational 0.17 µm, 0.12 µm and 0.10 µm. The experimental setup being a contact measurement could yield more accurate results. This discrepancy can be a result of the computational measurements not accommodating all the irregularities on the surface. Previous authors have indicated that the magnification could be a potential barrier to account for all surface irregularities [24]. The same observation was made in the R_v values in the two phases. Moreover, the two approaches are conducted randomly, potentially leading to variation in the R_a and R_v values.

Generally, the measured values are within the roughness standard developed by the International Standard Organisation (ISO 5436-1 type c) which indicates that R_a values should range from 0.1 µm to 10 µm, and R_v 0.1 µm to 20 µm [25]. In the transport sector, the R_a values are up to 3.20 µm and lower due to their exposure to harsh environments and dynamic loading [6]. It is inherent that high energy might have led to reduced powder spreading on the surface. This finding relates well with previous studies that have demonstrated that controlling the energy density, which is a function of hatch distance, scanning speed and laser power can result in satisfactory surface quality [7-9]. It was reported that depth valley can vary due to pores on the surface that emanate from pool shrinkage [5]. It is critical to ensure that the processing parameters result in dense parts, which helps achieve parts with better performance such as fatigue and corrosion.

The sample's microstructure can also be influenced through vibratory processing due to the interaction in the rotational shaft that creates friction [20]. Surface polishing for 3 hours ensures that at a lower speed, there is less debris that initiates defects on the surface. AlSi12 being a soft material, can achieve lower R_a better than harder metals under optimised

conditions of reduced friction and vibrations [8]. The R_a and polishing treatment relationship are not always linear, as demonstrated by the resulting graphs in Fig. 2 and 3.

It is inherent that the different speeds affected the sample surface after polishing; this revealed that a speed of 180 rpm in the two phases is conducive to the AlSi12 surface improvement as indicated by the lowest measured R_a values. However, the R_v value was lowest at a speed of 160 rpm, showing that the optimal speed for R_v can differ from that of R_a. In addition, the reduction in R_v was not as significant as the one in R_a values during the experimental measurements, while in the computational setup, the decrease was remarkable. This implies that there was a slight deformation on the surface due to material removal that affected the microstructure. The plastic media mixed with zirconia balls might have caused a realignment of the particles and grains on the surface during the repeated interaction in the tumbler. This provides complementary acumens with the vibratory polishing process smoothening the valleys and peaks of the surface morphology. Both in the experimental and computational measurements, the values of the R_a and R_v have decreased from the as-built condition. A surface with low R_a and high R_v might seem smooth surface but have an inconsistent structure that leads to defects such as cracks on the material in transport applications. This behaviour aligns with the fact that a high R_v might compromise the load bearing of the surface, consequently leading to premature failure [9].

5 Conclusion

In this study, the surface roughness in terms of the Ra and Rv have been investigated using both experimental and computational approaches. By analysing Ra and Rv in different phases, the findings of the study demonstrated that the plastic combined with the zirconia balls polishing media can have a considerable removal effect and enhance the surface roughness of the AlSi12 alloy. All the samples' surface roughness values obtained showed a decrease from the as-built condition. However, the measurements from the experimental and computational results presented some discrepancies in the last phase. This implies that both methods have shortfalls and can be complementary, as both are localised measurements. The use of the two methods provides a multifaced approach to effective decision-making for components with requirements of efficient mechanical properties and durability.

Further studies should analyse the effect of varying the polishing time and consider different energy densities to evaluate the machinability ranges of the material.

The authors acknowledge the Council for Scientific and Industrial Research, Laser Enabled Manufacturing Photonic Centre for the fabrication of samples. They also extend their appreciation to the Metallurgical Laboratory and Advanced Material Engineering (AME) where the polishing was conducted and the Surface Engineering Research Laboratory at the Tshwane University of Technology (TUT) for their assistance with the experiments. Special thanks are given of Mr Mandy Madigoe (AME) and Dr Dada Mudeopola (TUT) for their invaluable assistance.

References

[1] N.T. Aboulkhair, M. Simonelli, L. Parry, I. Ashcroft, C. Tuck, R. Hague, 3D printing of Aluminium alloys: Additive Manufacturing of Aluminium alloys using selective laser melting, Progress in materials science **106** (2019).
[2] S.T. Olohunde, A.M. Hafizi, I. Jamaliah, A.A. Al-Bakoosh, O.O. Segun, I.O. Sadiq, Corrosion Resistance of Aluminium–Silicon Hypereutectic Alloy from Scrap Metal, Journal of Bio- and Tribo-Corrosion 5(2) **41**, (2019).

[3] A. Boschetto, L. Bottini, F. Veniali, Roughness modeling of AlSi10Mg parts fabricated by selective laser melting, Journal of Materials Processing Technology. **241**,154-163 (2017).
[4] E.O. Olakanmi, R. Cochrane, K. Dalgarno, A review on selective laser sintering/melting (SLS/SLM) of aluminium alloy powders: Processing, microstructure, and properties, Progress in Materials Science **74**, 401-477 (2015).
[5] E. Yasa, Chapter 3 - Selective laser melting: principles and surface quality, in: J. Pou, A. Riveiro, J.P. Davim (Eds.), Additive Manufacturing, Elsevier2021, pp. 77-120.
[6] D. Greitemeier, F. Palm, F. Syassen, T. Melz, Fatigue performance of additive manufactured TiAl6V4 using electron and laser beam melting, International Journal of Fatigue 94 (2017) .
[7] A. Leon, E. Aghion, Effect of surface roughness on corrosion fatigue performance of AlSi10Mg alloy produced by Selective Laser Melting (SLM), Materials Characterization 131 (2017).
[8] N.E. Uzan, R. Shneck, O. Yeheskel, N. Frage, Fatigue of AlSi10Mg specimens fabricated by additive manufacturing selective laser melting (AM-SLM), Materials Science and Engineering: A 704 (2017).
[9] T. Yang, T. Liu, W. Liao, E. MacDonald, H. Wei, X. Chen, L. Jiang, The influence of process parameters on vertical surface roughness of the AlSi10Mg parts fabricated by selective laser melting, Journal of Materials Processing Technology 266 (2019)
[10] J. Sun, Y. Yang, Z. Yang, Study on surface roughness of selective laser melting Ti6Al4V based on powder characteristics, Zhongguo Jiguang/Chinese J. Lasers 43 (2016)
[11] B. Van Hooreweder, K. Lietaert, B. Neirinck, N. Lippiatt, M. Wevers, CoCr F75 scaffolds produced by additive manufacturing: Influence of chemical etching on powder removal and mechanical performance, Journal of the Mechanical Behavior of Biomedical Materials 68 (2017).
[12] V. Urlea, V. Brailovski, Electropolishing and electropolishing-related allowances for powder bed selectively laser-melted Ti-6Al-4V alloy components, Journal of Materials Processing Technology 242 (2017).
[13] A. Mohammad, M.K. Mohammed, A.M. Alahmari, Effect of laser ablation parameters on surface improvement of electron beam melted parts, The International Journal of Advanced Manufacturing Technology 87 (2016).
[14] B. AlMangour, J.-M. Yang, Improving the surface quality and mechanical properties by shot-peening of 17-4 stainless steel fabricated by additive manufacturing, Materials & Design 110 (2016).
[15] K.L. Tan, S.H. Yeo, Surface modification of additive manufactured components by ultrasonic cavitation abrasive finishing, Wear 378 (2017).
[16] A.W. Hashmi, H.S. Mali, A. Meena, M.F. Hashmi, N.D. Bokde, Surface Characteristics Measurement Using Computer Vision: A Review, CMES-Computer Modeling in Engineering & Sciences 135(2) (2023).
[17] D. Modupeola, P. Patricia, Surface Roughness Measurements of Laser Deposited AlCoCrFeNiTi and AlCoCrFeNiCu High Entropy Alloys for Aerospace Applications, TMS 2023 152nd Annual Meeting & Exhibition Supplemental Proceedings, Springer Nature Switzerland, Cham, (2023).
[18] Z. Liu, S. Liu, Y. Li, P.A. Meehan, Modeling and optimization of surface roughness in incremental sheet forming using a multi-objective function, Materials and Manufacturing Processes **29**, 7, (2014)
[19] S. Lee, B. Rasoolian, D.F. Silva, J.W. Pegues, N. Shamsaei, Surface roughness parameter and modeling for fatigue behavior of additive manufactured parts: A non-destructive data-driven approach, Additive Manufacturing 46 (2021).

[20] B.J. Mfusi, N.R. Mathe, N.W. Makoana, P. Popoola, Optimization of surface modification for additively manufactured AlSi10Mg using a vibratory polishing surface finisher, (2022).
[21] M. Butt, D. Ali, M. Aftab, M.U. Tanveer, Surface topography and structure of laser-treated high-purity zinc, Surface Topography: Metrology and Properties **3**, 3 (2015).
[22] W. Li, C. Wang, Z. Shi, Y. Wei, H. Zhou, K. Deng, The description of shale reservoir pore structure based on method of moments estimation, PloS one 11(3) (2016) e0151631.
[23] Y. Hao, S. Yang, X. Li, W. Li, X. Wang, Analysis of contact force characteristics of vibratory finishing within pipe-cavity, Granular Matter 23 (2021).
[24] S.R. Yadhuraj, G. Satheesh Babu, M. Uttara Kumari, *Measurement of thickness and roughness using gwyddion*, 2016 3rd International Conference on Advanced Computing and Communication Systems (ICACCS), (2016).
[25] F. Saraiva, P. Neves, C. Pires, J.A. Sousa, A novel traceability route to the SI in roughness measurements at IPQ, Acta IMEKO **12**, 3 (2023).